Deep Cerebellar Stimulation Reduces Ataxic Motor Symptoms in the *Shaker* Rat

Collin J. Anderson, PhD,[1] Karla P. Figueroa, MS,[1] Alan D. Dorval, PhD,[2] and Stefan M. Pulst, MD, DrMed[1]

Objective: Degenerative cerebellar ataxias (DCAs) affect up to 1 in 5,000 people worldwide, leading to incoordination, tremor, and falls. Loss of Purkinje cells, nearly universal across DCAs, dysregulates the dentatothalamocortical network. To address the paucity of treatment strategies, we developed an electrical stimulation-based therapy for DCAs targeting the dorsal dentate nucleus.
Methods: We tested this therapeutic strategy in the Wistar Furth *shaker* rat model of Purkinje cell loss resulting in tremor and ataxia. We implanted *shaker* rats with stimulating electrodes targeted to the dorsal dentate nucleus and tested a spectrum of frequencies ranging from 4 to 180 Hz.
Results: Stimulation at 30 Hz most effectively reduced motor symptoms. Stimulation frequencies >100 Hz, commonly used for parkinsonism and essential tremor, worsened incoordination, and frequencies within the tremor physiologic range may worsen tremor.
Interpretation: Low-frequency deep cerebellar stimulation may provide a novel strategy for treating motor symptoms of degenerative cerebellar ataxias.

ANN NEUROL 2019;85:681–690

Degenerative cerebellar ataxias (DCAs) affect 1 in 5,000 individuals,[1] and their motor symptoms frequently include gait incoordination, tremor, and falls. DCAs have numerous etiologies, Mendelian and sporadic. Despite 20 years having passed since spinocerebellar ataxia–causing genes were first identified,[2,3] treatment strategies remain limited. Therapeutic approaches vary,[4] but they typically fail to sufficiently alleviate symptoms.[5–9] Most degenerative ataxias feature Purkinje cell loss,[10,11] resulting in modified inputs to the deep cerebellar nuclei; thus, neuromodulation targeting these deep cerebellar nuclei may succeed in numerous DCAs.

Deep brain stimulation (DBS) in the deep cerebellar nuclei, downstream from degenerating Purkinje cells, may ameliorate the effects of Purkinje cell loss. Whereas previous work assessed thalamic and basal ganglia stimulation to treat DCAs,[12,13] we targeted stimulation to the dorsal dentate nucleus, because the dentate is immediately downstream from Purkinje cells; furthermore, as the primary cerebellar motor output, it processes the majority of deep cerebellar motor control information. Although deep cerebellar stimulation (DCS) is novel for DCAs, it can yield therapeutic changes in the context of spasticity[14] and recovery from stroke.[15–17]

We tested whether dorsal dentate nucleus electrical stimulation reduces degenerative ataxia motor symptoms using the Wistar Furth *shaker* rat, an x-linked recessive DCA model. *Shaker* rats progressively lose Purkinje cells but retain an intact overall cerebellar architecture and dentatothalamocortical pathway.[18,19] Symptoms begin at ~9 weeks with a full-body tremor, progressing to a severe, shaking ataxia, with frequent falling. The *shaker* rat's recapitulation of the salient features of DCAs, its large cerebellar targets, and the high-throughput nature of rodent experiments made it ideal for these studies. We adapted a center of mass tracking design[20] and wrote custom software to directly measure tremor, gait coordination, and falls in an automated, operator-independent fashion. We tracked symptom presentation in *shaker* and wild-type (WT) rats from which to compare symptom progression and determined baselines and appropriate ages for symptom analysis.

View this article online at wileyonlinelibrary.com. DOI: 10.1002/ana.25464
Received Aug 30, 2018, and in revised form Mar 6, 2019. Accepted for publication Mar 7, 2019.
Address correspondence to Dr Anderson, Department of Neurology, University of Utah, Salt Lake City, UT 84112. E-mail: collina@genetics.utah.edu
From the [1]Department of Neurology and [2]Department of Bioengineering, University of Utah, Salt Lake City, UT
Additional supporting information can be found in the online version of this article.

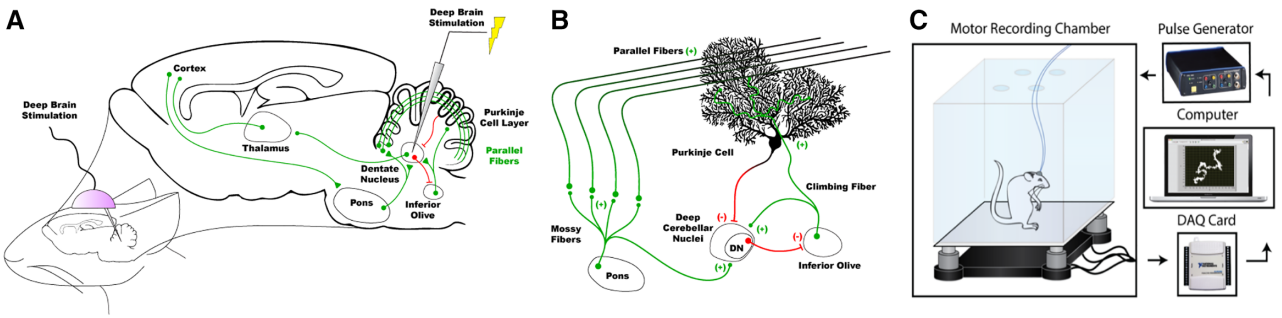

FIGURE 1: Network model and experimental setup. (A) The dentate nucleus receives inhibitory input from Purkinje cells, progressively lost in the *shaker* rat model, and excitatory input from mossy and climbing fiber collaterals from pons and inferior olive. (B) Short-term Purkinje cell disinhibition facilitates movement dentate bursting and consequent movement. We hypothesized that, in the absence of Purkinje cells, the dentate cannot respond properly to excitatory collateral inputs. Whereas Purkinje cell millisecond-scale timing is likely necessary for fine motor control, we proposed that enhancing the dentate's ability to respond to excitatory collateral inputs may assist with less precise coordination, such as with gait. DN = dentate nucleus. (C) Cartoon of data collection setup. Load cells interface through a DAQ card to LabVIEW for power and to provide data to quantify center of mass in real time at 1,000 Hz. The pulse generator provides electrical stimulation to the rat through a tether.

Therapeutic electrical stimulation frequencies vary across neurological diseases. Parkinsonian DBS is usually >100 Hz, although 60 Hz can effectively treat bradykinesia.[21] Ten-kilohertz stimulation is effective for spinal cord stimulation for chronic leg and back pain,[22] and sub-50 Hz stimulation can be effective for stroke recovery,[15,16] chronic pain,[23] and catalepsy.[24] Certain parameters improve some symptoms while worsening others; high-frequency stimulation for primary parkinsonism symptoms exacerbates vocalization deficits.[25,26] We hypothesized that low-frequency stimulation would be most effective for ataxia because low-frequency stimulation enhances network throughput,[16,27] whereas high-frequency stimulation functions as an informational lesion.[28–30]

Thus, we tested frequencies from 4 to 180 Hz. We found 30 Hz to be most effective, whereas substantially lower or higher frequencies may worsen specific symptoms. Given that DBS effects can change over long periods, such as in dystonia treatment,[31] we tested the effects of stimulation over several hours and found them to hold.

DCS may offer the rare chance to improve gait ataxia. Beyond presenting a new therapeutic option and new tools for ataxia study, our work is relevant to ongoing discussions of DBS mechanism and should encourage researchers to attempt low frequencies in novel DBS uses when symptoms may emerge from a neurological loss of information.

Materials and Methods

All surgical and experimental procedures were performed in the Department of Neurology at the University of Utah, were approved by the institutional animal care and use committee of the University of Utah, and complied with US Public Health Service policy on the care and use of laboratory animals.

Experimental Protocols

We collected center of mass data in several cohorts of awake, unrestrained Wistar Furth rats (Fig 1C). First, we recorded 6 *shaker* rats and 4 WT rats weekly from 7 to 35 weeks of age. Second, we surgically implanted 7 *shaker* rats with chronic, bilateral, stimulating electrodes targeted to the dorsal dentate nucleus at 18 to 19 weeks of age and recorded repeatedly under various conditions from 20 to 28 weeks of age (see Fig 1A, B). Center of mass data were collected from this cohort both on and off stimulation. After recordings, we perfused rats with phosphate buffer solution through the cardiovascular system and fixed with 4% paraformaldehyde before taking cerebella for histological analysis. Numbers of rats included in stimulating experiments were based on power analysis from preliminary data based on $\alpha = 0.05$, power of 0.9, and a prediction of ~25% surgical or electrode failure.

Motor Analysis. We created custom LabVIEW software to track center of mass at high frequency, based on previous work quantifying rodent center of mass by Fowler et al.[20] We attached a 1 cubic foot Plexiglas enclosure to the recording counter and centered 4 Honeywell (Morristown, NJ) model 31 miniature load cells under the corners of the Plexiglas enclosure, each attached to the corner of a 35-pound granite ballast (see Fig 1A). We placed a rigid, sub-100 g detachable platform on the load cells below the bottom of the Plexiglas enclosure. We made a 2 cm hole on top of the chamber to allow tether connection. We soldered load cell inputs and outputs to a National Instruments (Austin, TX) USB-6008 DAQ interface for powering cells and collecting voltages.

We sampled load cell voltages at 1,000 Hz in LabVIEW and computed position based on the weighted averages of forces applied at each of the load cells and their respective positions.[20] We exported positional data to MATLAB (MathWorks, Natick, MA) and wrote MATLAB code to analyze tremor, straightness of gait, and fall rates.

We analyzed tremor through position data Fourier analysis. Tremor frequencies observed during preliminary data collection were typically 2.5 to 8 Hz. Thus, we conservatively analyzed tremor from 2 to 10 Hz. We computed Fourier transforms of position over successive 5-second time intervals, averaged the Fourier transforms of age-matched WT rats, and integrated the area between the affected rat's Fourier transforms and the average of those from age-matched WT rats from 2 to 10 Hz. We normalized this value on a scale with 0 as WT average and 1 as the highest within-group weekly average for *shaker* rats.

We computed straightness of gait as an incoordination surrogate. Distances traveled over a threshold of 8 mm in 1 second were autodetected and analyzed for straightness of gait. Importantly, the specific threshold was unimportant: we repeated analyses with a number of thresholds and found results to be similar across thresholds. We chose 8 mm as it was sufficiently large to eliminate shifts in weight but not too great to eliminate movements in which a turn was being made. For each movement, we computed the net displacement of the movement and the total distance traveled, sampled at 20 Hz. We computed the ratio of total movement distance to net displacement, thus giving an index for straightness of gait. A perfectly straight ambulation would give a ratio of exactly 1—which is not achievable, as a minor amount of sway will be present in even healthy animals as they alternate feet—and a particularly uncoordinated movement with a great deal of truncal sway might yield a value of ~3.

We automated the detection of falls by identifying large millisecond-scale changes in force applied to load cells, only present during falls. During falls, the abrupt impulse applied to the nonaffixed platform would deweight at least one load cell for a duration of several milliseconds, providing a brief change in the force to that cell much more rapidly than could be caused by the most rapid movements made by rats. We tested various force thresholds and selected one that maximized agreement with qualitative fall determination, with 95 + % agreement between automated detection and observed falls.

For all quantified measures, we measured the effects of DCS in a normalized fashion. As the data to be collected were numerous enough to require a minimum of several weeks of data collection time, and the motor symptoms in the *shaker* rat are constantly evolving, we alternated recordings on- and off-stimulation, with the first condition randomly chosen, and normalized on-stimulation symptom severity to off-stimulation averages made on the same day. For each symptom, we normalized such that a value of zero matched the average value collected from age-matched WTs, and a value of 1 matched the average value collected during sham stimulation, that is, with stimulation turned off and symptoms untreated.

Surgical Procedures. We subcutaneously administered rats 0.01 mg/kg Buprenex. After a 2-hour wait, we anesthetized with 1 to 2% isoflurane. We shaved and disinfected the surgical site and placed rats on a heating pad in a stereotactic frame. We administered 0.1 ml bupivacaine to the incision site, and then opened to the scalp and dried. We marked craniotomy sites with respect to bregma.[32] We used a burr to drill 7 holes anterior to the craniotomy sites and placed 7 titanium bone screws to anchor eventual implants. We bilaterally targeted microelectrodes to the dorsal dentate nuclei. Given that craniotomies more than ~10 mm posterior from bregma induced bleeding in preliminary studies, we targeted through burr holes 9.5 mm and 3.5 mm lateral from bregma and then angled electrodes through 6.1 mm at 14.3° to reach their target (3.5 mm lateral, 11.0 mm posterior, 5.9 mm ventral from bregma). We implanted 2-channel microstimulating arrays—75 μm platinum–iridium electrodes with 200 μm center-to-center spacing from Microprobes for Life Science (Gaithersburg, MD)—through the holes and cemented them to the bone screws with dental acrylic. After placing all elements, we smoothed over the headcap with additional acrylic. We sutured the incision and provided 0.1 mg/kg carprofen subcutaneously 3 times daily following implantation. Rats were given a 2-week recovery period.

Deep Cerebellar Stimulation. For all implanted animal trials, whether stimulation was provided or not, we attached a 2-channel tether to each of the array connectors on the headcap. We fed the tether through the top of the behavioral chamber to a commutator and connected the commutator to a pulse generator (see Fig 1B). We determined amplitude thresholds by gradually increasing current until side effects occurred, ranging from whisker twitching and sudden movements to full-body muscular contractions. We set current to 90% of the minimum that induced side effects, with a conservative maximum of 250 μA, based on computing a safe current ceiling of 300 μA.[33] We delivered bipolar, biphasic stimulation with 100-microsecond pulse width. We applied stimulation for 5 minutes prior to on-DCS recordings and turned it off for 5 minutes prior to off-DCS recordings.

Motor Recordings. We made weekly 30-minute recordings in 6 *shaker* rats and 4 WT rats 7 to 35 weeks old, demonstrating that the quantified symptoms were present in all *shakers* by 19 weeks. Thus, we collected motor data from array-implanted *shaker* rats between 20 and 29 weeks old, ensuring the presence of all symptoms. Several factors necessitated within-day normalization when quantifying symptom alleviation. First, symptoms evolve in the *shaker* rat model and recordings lasted a number of weeks, sufficiently long for substantial evolution. Second, repeated recordings reduced environment novelty, potentially reducing exploratory behavior. Finally, we observed adaptive behaviors by *shaker* rats—using walls for support, wider stance, etc—and could

not discount progressive adaptation in the chamber over successive recordings.

While testing DCS, we made recordings during 40-minute intervals, alternating on- and off-stimulation, randomly selecting whether to first record on or off DCS, preventing bias from on versus off order. We normalized symptoms recorded with stimulation to values recorded without stimulation during the same interval. In each scenario, we allowed 5 minutes in the stimulation setting—on or off—before collecting motor data for 5 minutes, avoiding wash-on and wash-off effects. Following the collection of motor data at all tested DCS frequencies—4, 10, 20, 30, 40, 60, 80, 100, 130, and 180 Hz—we tested the effects of the most effective frequency, 30 Hz, over a longer duration to ensure that the effects of stimulation would still be present, at least over a moderate time scale. On 2 successive days, starting within 10 minutes of the same time of day, rats were placed in the recording box for 2 hours with stimulation turned on or off—with random selection as to which recording was made first—and then recorded for 15 minutes in the condition. Thus, rats were recorded during the final 15 minutes of a 2-hour, 15-minute session in the motor recording chamber either with stimulation the full time or no stimulation provided at any point.

Histology. Following data collection, we anesthetized rats, perfused through the cardiovascular system with phosphate-buffered saline, fixed with 4% paraformaldehyde (PFA), and removed cerebella. We soaked cerebella in 4% PFA, cryoprotected, and flash froze each in OCT compound before cutting into 25 μm coronal slices with a Leica (Wetzlar, Germany) 5100 s cryostat. Finally, we located electrode tracts and estimate electrode tip locations.

Statistical Analysis. When data were distributed in an approximately Gaussian fashion, summary values consist of mean and standard error. When data were distributed in a non-Gaussian fashion, we found summary values from 100,000 bootstrapped populations resampled with replacement and present means and inner quartiles. Statistical test abbreviations consist of *t* test as Student *t* test and *bca* as bootstrapped confidence assessment. When multiple frequencies were compared to sham stimulation and when multiple ages of animals were, significance was determined from $\alpha = 0.05$ following Holm–Bonferroni multiple comparison correction; resulting nominal and corrected *p* values are listed.

Results

Ten rats, 6 *shaker* and 4 WT, made motor recordings weekly from 7 to 35 weeks of age. Eight 17–18 week *shaker* rats were bilaterally implanted with stimulating arrays targeted to the dorsal dentate nucleus, and 7 survived surgery. The electrode headcaps dislodged from 2 rats during the course of experimentation. All rats were tested at both 30 Hz—the most effective frequency—prior to headcap loss.

Model Characterization

Tremor emerges strongly with symptom onset. We compared tremor, straightness of gait, and fall rates between *shaker* and WT rats at 7 to 35 weeks of age (Fig 2). In all *shaker* rats, tremor presented either first or alongside other symptoms. Four rats exhibited tremor at 9 to 11 weeks of age, the last 2 having symptom onset at 14 and 19 weeks. These were consistent with previous qualitative determinations that *shaker* rats first display symptoms between 9 and 20 weeks of age.[18] Whereas qualitative observations noted onset no earlier than 9 weeks, we quantitatively found that *shaker* rats demonstrated significantly more tremor than WT animals (*bca*, $p < 0.00001$) at all ages from 8 weeks on. Power spectra of representative 10-week *shaker* and WT rats are shown (see Fig 2A), along with tremor versus age (see Fig 2B).

Incoordination of gait progresses more slowly. Representative movements made by 24-week *shakers* and WTs depict *shaker* rat truncal sway as they fail to travel in a straight line (see Fig 2C). *Shaker* rats walked straighter at 7 weeks (*bca*, $p = 0.0033$), but gait trended less straight for several months before stabilizing, with less straight gait than WT rats at 10+ weeks (see Fig 2D; *bca*, $p < 0.0002$ at all 10+ week ages).

Fall rate progression largely follows incoordination of gait. Finally, whereas *shaker* rats fell less than WT animals at 7 weeks of age (*bca*, $p = 0.0050$), they fell more frequently at 9+ weeks of age (*bca*, $p = 0.043$ at 9 weeks of age, $p < 0.03$ at all ages beyond 9 weeks). Similar to straightness of gait, fall rates trended worse for several months before stabilizing (see Fig 2E).

Deep Cerebellar Stimulation

Thirty-hertz DCS reduces symptom severity on an acute timescale. We acutely tested DCS in 20- to 28-week *shaker* rats. We normalized on-condition recordings to off-condition recordings from the same day. In general, 30 Hz DCS was most effective. Tremor was significantly reduced by 10, 20, and 30 Hz stimulation (Fig 3A; *bca*, $p < 0.0022$ nominal for each, $p < 0.018$ corrected). Forty-hertz trended toward reduced tremor (*bca*, $p = 0.012$ nominal, not significant corrected), 4 Hz stimulation trended toward worsened tremor (*bca*, $p = 0.030$ nominal, not significant corrected), and 60+ Hz stimulation had little to no effect. Gait was significantly straightened by 20 and 30 Hz stimulation (see Fig 3B; *bca*, $p < 0.0049$ nominal for each, $p < 0.044$ corrected), whereas other frequencies up to 100 Hz had little to no effect. One hundred thirty–hertz and 180 Hz stimulation, used for parkinsonism and essential tremor, trended toward worsened gait (*bca*, $p = 0.013$ and $p = 0.092$ nominal, respectively, not significant corrected). Analyzing 130 Hz and 180 Hz together

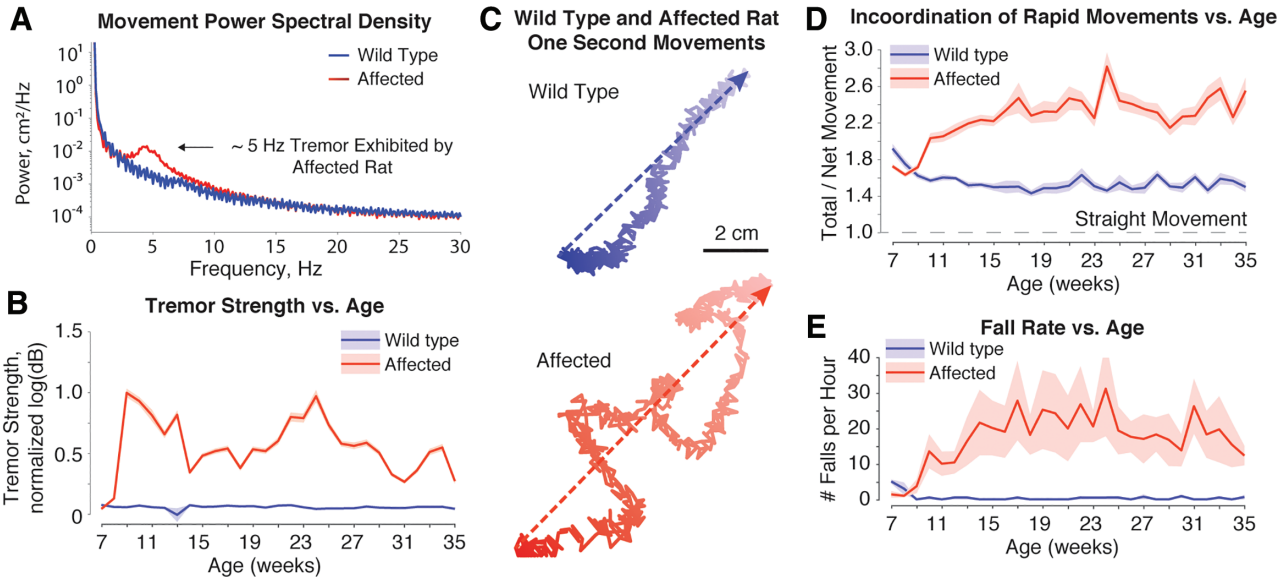

FIGURE 2: Quantification of motor symptoms in the Wistar Furth *shaker* rat. (A) Power spectral densities of center of mass tracking data for 10-week-old wild-type (WT; blue) and *shaker* (red) Wistar Furth rats. The ~5 Hz peak in the *shaker* rat indicates ~5 Hz tremor. (B) Tremor, measured across 2 to 10 Hz, was greater in affected animals than in WT animals at 8 weeks and beyond (*bca*, $p < 0.00001$). Lighter color indicates bootstrapped inner quartiles in B, D, E. (C) Age-matched, 26-week-old WT (blue) and *shaker* (red) rat center of mass traces during rapid movements. Color changes from dark to light indicate 1-second change in time; dashed arrows denote displacement. WT animals made straighter movements. (D) Comparing total distance traveled during rapid movements versus net movement displacement, affected rats demonstrated progressive incoordination and were significantly less coordinated than control animals at all time points after 9 weeks (*bca*, all $p < 0.0002$). (E) Affected rats fall significantly more than WT rats at 9+ weeks (*bca*, all $p < 0.03$).

based on their likely similar neural effect yielded worsening of gait (*bca*, $p = 0.0048$ nominal, $p = 0.043$ corrected). Thirty-hertz stimulation reduced falling (see Fig 3C; *bca*, $p = 0.00021$ nominal, $p = 0.0021$ corrected), whereas 40 Hz stimulation trended toward improvement (*bca*, $p = 0.038$ nominal, not significant corrected).

With each rat, at each frequency, we determined minimum amplitudes that induced side effects, testing stimulation at 90% of this threshold. Interestingly, we found the relationship between current threshold and frequency to approximately resemble that of a strength-duration curve, only with frequency on the x-axis rather than pulse width (see Fig 3D). One rat did not exhibit side effects at any amplitude and frequency combination, but it has not been excluded from analyses, except from the side effect threshold plot.

Thirty-hertz stimulation is still effective on a moderate timescale. After testing all frequencies, we tested 30 Hz DCS over a moderate timescale. We compared on-stimulation versus off-stimulation conditions over back-to-back days at the same time of day, making 15-minute recordings after rats spent 2 hours tethered and within the specified condition, order of presentation randomized. In terms of tremor (Fig 4A; *bca*, $p = 0.0117$) and straightness of gait (see Fig 4B; *bca*, $p = 0.0404$), 30 Hz stimulation significantly improved symptoms after being applied for 2 hours. In terms of falls, 30 Hz stimulation trended toward improved symptoms, but changes were insignificant (see Fig 4C), with limited data points and large variability.

Histological Analysis

Rats with electrodes implanted in or near the dentate nucleus received treatment benefit. We cut cerebella into 20 µm slices and localized 12 of 14 electrode tracts (Fig 5). We found that all but 3 electrode tips were estimated to be within 500 µm of the dorsal dentate nucleus, at which point the dorsal dentate nucleus would be largely activated by 250 µA stimulation from our electrodes. One animal demonstrated no side effects at any combination with both electrodes located an estimated 1+ mm from the target, and 1 animal had 1 electrode ~1 mm from the target but another within 200 µm, demonstrating side effect thresholds consistent with other animals and therapeutic benefit, indicating that unilateral stimulation may be useful. Finally, half of electrodes localized would likely have activated at least a portion of the dorsolateral interposed nucleus.

Discussion

DBS is clinically established to treat medically refractory forms of several neurological diseases, but DBS for cerebellar disorders has not been studied extensively. This work demonstrates that DCS may provide a novel therapeutic strategy in ataxia treatment. We used a unique genetic rodent model with progressive Purkinje cell degeneration, allowing precise disease process timing and obvious symptoms. Using a rat rather than

mouse model made targeting more reliable, allowing us to observe improvement in motor phenotypes. Furthermore, using a rodent model gave us the opportunity to test many frequencies, with multiple trials per frequency per animal, to more precisely determine the effects of stimulation.

Comparison with Pharmaceutical Strategies

It is possible that therapeutic effects could be stronger in humans, with better electrode targeting programming. DCS, if translated, may prove a more widely useful therapeutic strategy than pharmaceutical approaches. Arguably the most promising pharmaceutical approach proposed for ataxias is antisense oligonucleotides (ASOs).[34,35] Although ASOs will likely prove more beneficial than DCS for patients with specific ataxias for which ASOs exist, patients with sporadic ataxias, spinocerebellar ataxias without an ASO, or hereditary ataxias for which the gene is unknown cannot benefit from ASOs. In many of these cases, patients could be DCS candidates. Although it is unreasonable to hypothesize that DCS will slow disease progression or resolve very fine motor control symptoms, it may provide substantial gait ataxia relief.

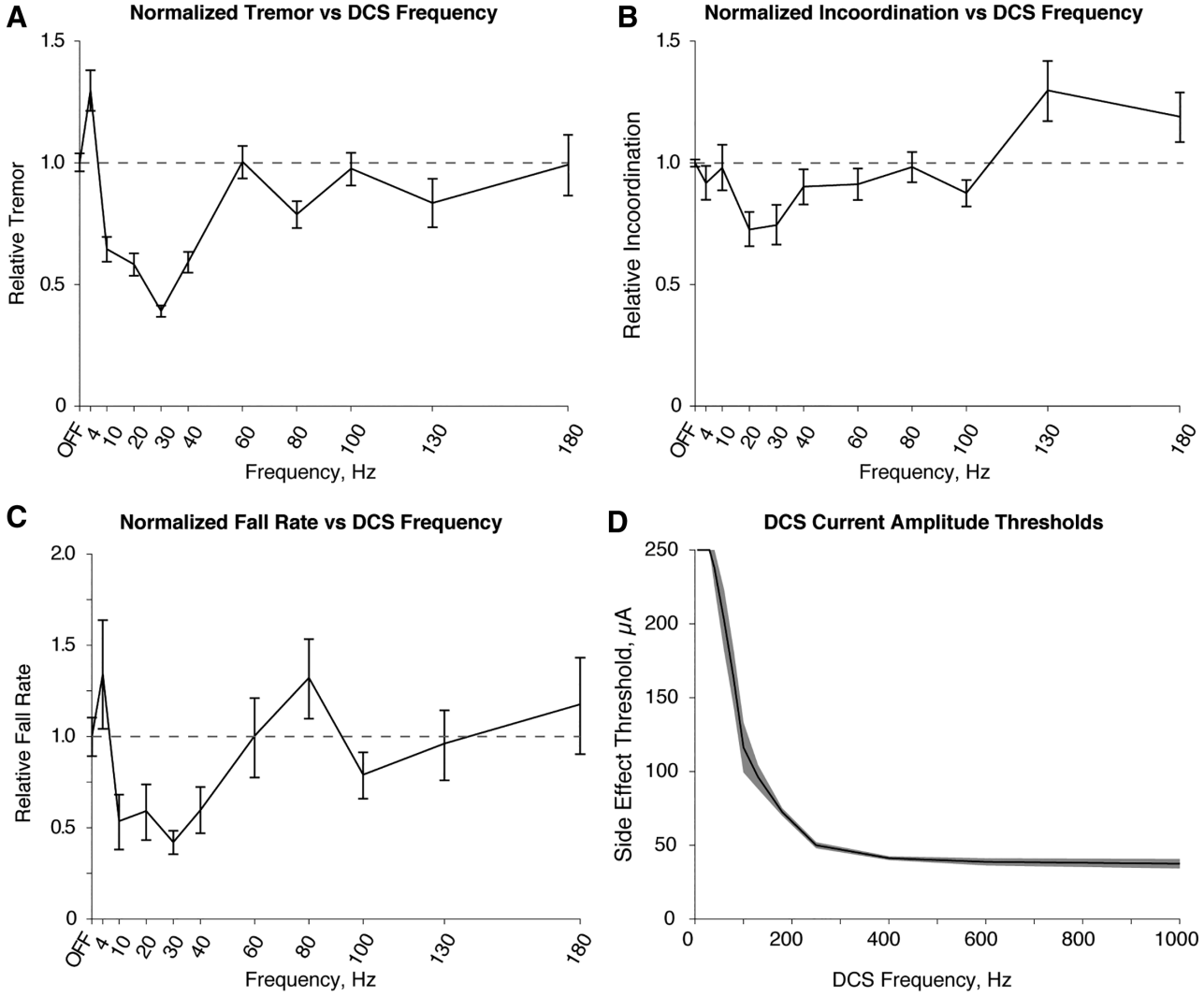

FIGURE 3: Effects of deep cerebellar stimulation (DCS) on motor symptoms; side effect thresholds versus frequency. Error bars in A–C and gray in D represent bootstrapped middle quartiles. (A) Ten-, 20-, and 30 Hz stimulation resulted in tremor reduction (*bca*, $p < 0.005$ nominal, $p < 0.05$ corrected), and 40 Hz stimulation trended toward improvement (*bca*, $p = 0.0116$ nominal, not significant corrected). Four-hertz stimulation trended toward worsened tremor (*bca*, $p = 0.0304$ nominal, not significant corrected), and 60+ Hz stimulation had no significant effect. (B) Twenty- and 30 Hz stimulation improved straightness of gait (*bca*, $p < 0.005$ nominal, $p < 0.05$ corrected); 130- and 180 Hz stimulation, individually, trended toward worsened incoordination, but had a combined significant effect of increased incoordination (*bca*, $p = 0.00447$ nominal, $p < 0.05$ corrected). (C) Thirty-hertz stimulation resulted in reduced fall rates (*bca*, $p = 0.00021$ nominal, $p < 0.05$ corrected). (D) Higher stimulation frequencies resulted in motor side effects with lower amplitudes. To avoid damage to neural tissue, we did not test amplitudes higher than 250 μA. Whereas no rats were excluded from A–C, 1 rat was excluded from D due to both exhibiting no side effects at any frequency–amplitude combination and having both electrodes well off target (see Fig 5).

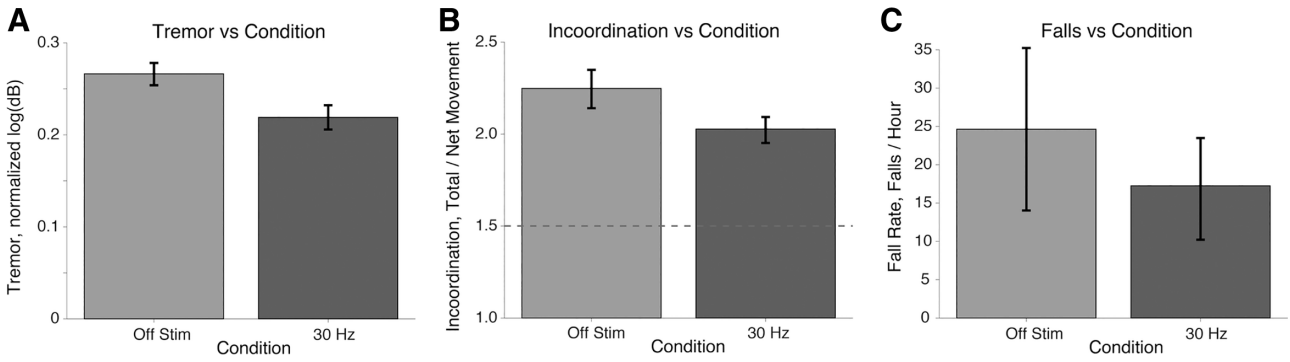

FIGURE 4: Thirty-hertz stimulation maintains efficacy over a longer timeframe. Thirty-hertz and sham stimulation were presented for a period of 2.25 hours on back-to-back days, starting at the same time of day, order of presentation randomized. Motor recordings were made during the last 15 minutes and compared between groups. Error bars refer to bootstrapped middle quartiles. (A) Tremor is significantly lessened by 30 Hz stimulation after 2 hours stimulation duration (*bca*, $p = 0.0117$). (B) Gait is significantly straightened by 30 Hz stimulation after 2 hours stimulation duration (*bca*, $p = 0.0404$). Note that a value of 1.0 refers to perfectly straight gait, whereas wild-type rats average a value of approximately 1.5. (C) Fall rates trended positively with the application of 30 Hz stimulation after 2 hours duration, but were not significantly improved.

Low-frequency stimulation may function through network enhancement. Parkinsonism and essential tremor are typically treated with high-frequency stimulation.[36] However, our work indicates that lower frequencies would be more effective in the treatment of ataxia. High-frequency DBS functions as an informational lesion[28,29] or functional deafferentation,[37] whereas it has been proposed that low-frequency (<50 Hz) stimulation enhances network output.[16,27] Purkinje cells regulate movement timing and strength through connectivity with the deep cerebellum, and complete suppression of Purkinje cells suppresses motor activity.[38] Thus, whereas parkinsonism is treated by informational lesion,[29] degenerative ataxias may require network enhancement. In this model, DCS enhances the passage of remaining coordination-relevant information

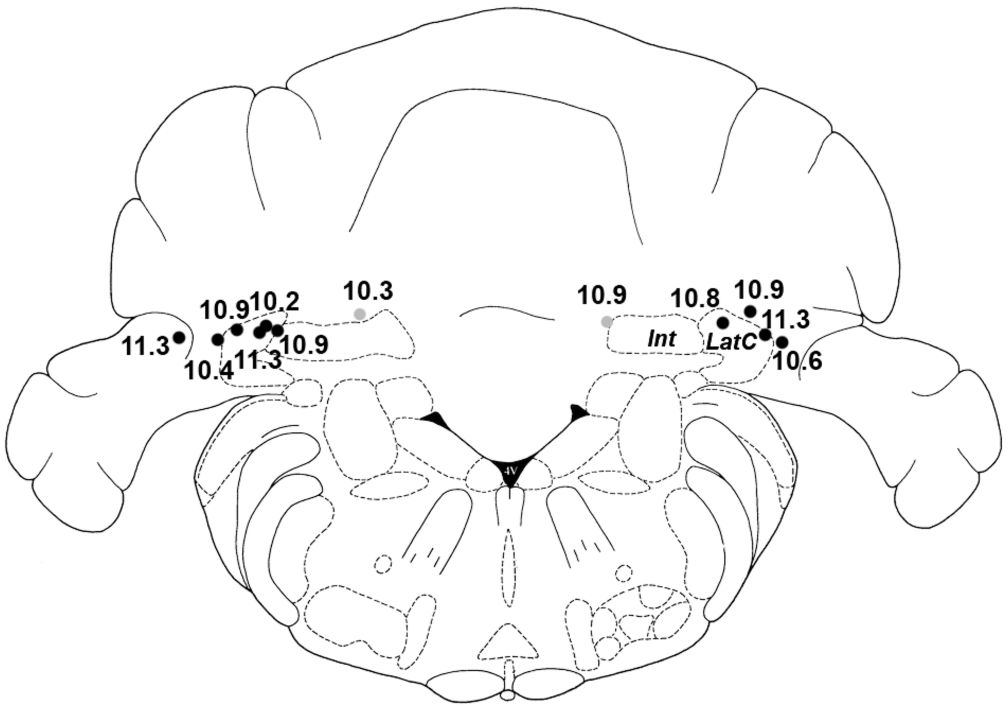

FIGURE 5: Electrode tip location estimates. The figure was adapted from Paxinos and Watson,[32] based on coronal slicing, 11.3 mm posterior from bregma, with dentate nucleus situated approximately 10.6 to 11.7 mm posterior from bregma. Electrode tracts were identified histologically, and tip locations were estimated and diagrammed. Numbers correspond to approximate distance of tip posterior from bregma in millimeters. Note that LatC refers to the lateral cerebellar nucleus, synonymous with dentate nucleus, whereas Int refers to interposed nucleus. For 6 animals in which stimulation produced side effects, 10 of the 12 electrode tracts were identified, and tip estimates are shown in black. For 1 animal in which stimulation did not generate side effects, both electrode tracts were identified, and tip estimates are shown in gray. Adapted from Paxinos and Watson,[32] with permission from Elsevier.

through the dentate, perhaps primarily through pontine mossy fiber and olivary climbing fiber collaterals. This could make sense given that low-frequency DBS increases firing variability and informational capacity.[39]

Very low- and high-frequency stimulation may worsen symptoms. Although low-frequency stimulation was most effective, very low frequencies in the range of tremor frequency may worsen tremor. Local field recordings in macaques have implicated deep cerebellar oscillations in tremor generation, with the frequency of oscillations corresponding to the frequency of tremor, and coherence between local fields potentials and finger acceleration.[40] Thus, introducing further tremor-frequency–range oscillations to the region may increase drive of tremor. On the other end of the frequency range, high-frequency stimulation did not significantly modify tremor, but frequencies >100 Hz may worsen incoordination. It is possible that high-frequency stimulation further blocks collateral signals while ineffectively reducing low-frequency oscillatory power, perhaps due to low side effect thresholds at high frequencies. This could explain the contrast to parkinsonian DBS, in which high-frequency stimulation reduces low-frequency oscillations.[41]

Stimulation of Deep Cerebellar Nuclei Versus Other Targets for Ataxia

Previous studies in ataxia patients showed that thalamic and basal ganglia stimulation improved cerebellar tremor, without consistently improving gait ataxia.[12,13] We propose that it may be possible to treat tremor through a wide set of stimulation locations and parameters, whereas improving coordination is more difficult. Inspired by the ideas that essential tremor depends on interplay across many oscillatory regions and may represent an intermediate state of Purkinje cell degeneration,[42] we propose that Purkinje cell misfiring and loss dysregulate the cerebellothalamocortical network, allowing oscillatory propagation through the network. It stands to reason that tremor generation could be disrupted at numerous nodes. However, movement coordination depends on the deep cerebellar nuclei. Purkinje cell loss directly reduces not only informational input, but also the dentate's ability to respond to collateral input through lost short-term disinhibition. As mossy fibers are too few[43] and climbing fibers are too slow[44] to generate the dentate bursting that precedes movement, short-term disinhibition from Purkinje cells facilitates bursting activity[45] and movement.[46] The absence of Purkinje cells may prevent short-term disinhibition and replace it with functionally dissimilar chronic disinhibition. Thus, low-frequency stimulation may aid in the propagation of coordination-relevant signaling from collaterals in the absence of short-term disinhibition. A single climbing fiber collateral arborization spreads several hundred micrometers within the rat dentate,[47] appropriate for generating coordination. In this interpretation, stimulation downstream from the deep cerebellar nuclei would not improve signal propagation through the deep cerebellum, hence the lack of gait ataxia improvement.

Finally, in the discussion of DBS of other targets in the context of ataxia, it is important to touch on pulse width modulation. Recent work indicates the great potential of pulse width shortening to avoid ataxic side effects in essential tremor patients with thalamic high-frequency stimulation, downstream from the deep cerebellum.[48] In this work, we chose to perform studies with a relatively long pulse width to increase the volume of tissue activated, as high-frequency and low-frequency DBS having substantially different effects on neural circuits and information processing, it is unlikely that low-frequency long-pulse stimulation will generate motor side effects, as confirmed by other rodent DCS studies.[16,17] However, given the recent work by Choe et al,[48] it will be important in the future to optimize stimulation in terms of not just frequency and amplitude, but also pulse width.

Stimulation Frequency Versus Side Effect Amplitude Threshold and Mechanisms

The relationship between stimulation frequency and side effect threshold hints at the importance of pacing of inputs to the deep cerebellar nuclei, especially given that Purkinje cell firing rate changes parallel motor symptom evolution prior to Purkinje cell loss.[49] It is possible that high-frequency stimulation may easily induce something akin to the bursting that assists with movement generation. The side effect profile typically observed with overstimulation comprises simultaneous contractions of multiple muscle groups, consistent with overexciting motor circuits. With lower frequencies, the amplitude required to produce enough excitatory input to generate unintended muscular contraction raises due to a reduction in stimulation rate. Although we did not determine stimulation thresholds at frequencies >1 kHz, it would be interesting to determine whether there is a horizontal asymptote or whether the relationship resembles a higher-order polynomial, as in the case of ultra–high-frequency thalamic stimulation losing efficacy in regularizing firing and suppressing tremor.[50] If the latter, it could be that the low- versus high-frequency stimulation mechanisms are similar in the deep cerebellar nuclei to those in the basal ganglia, thalamus, etc. The correct frequency choice for DBS treatment for a particular disease would simply depend on whether symptoms are generated primarily by gain of function, requiring high-frequency stimulation, or loss of function, requiring low-frequency stimulation.

Potential Caveats

We have only demonstrated improvements in ataxia specific to gait. It seems unlikely that the complex millisecond-timescale computations performed by Purkinje cells required for very

fine motor control—enabling, say, piano performance—can be recovered through electrical stimulation. However, gait ataxia improvement alone would represent a substantial improvement in patient treatment. Finally, based on relatively poor precision of bregma-based electrode targeting in rodent models, it is possible that the dentate nucleus was not the sole activated nucleus in all rats, and the interposed nucleus was likely activated in some. Given similar downstream regions activated by interposed and dentate, and related functions, it is reasonable to propose the interposed nuclei as a target. Future studies must be performed to determine whether it is ideal to stimulate in both or only the dentate. Finally, we must note that it is, of course, difficult to fully differentiate tremor from ataxia, as previous groups studying potential DBS therapies have noted.[13] A full-body tremor could seemingly result in an increase in our ataxia measure. However, comparison of the tremor versus ataxia plots in both Figures 2 and 3 clearly indicates that the tremor and ataxia measures are independent, as they evolve quite differently with age and frequency of stimulation.

It is clear that more study of low-frequency DCS to treat ataxias is warranted. Additional rodent work must be completed, but given the poor current treatment options, this therapeutic strategy may hold promise for numerous patients in the future.

Acknowledgment

This work was supported by grants R21NS10479901, R37NS03312317, and U01NS10388301 from the NIH National Institute of Neurological Disorders and Stroke to S.M.P, National Science Foundation NSF-CAREER 1351112 to A.D.D., a Utah Neuroscience Initiative Collaborative Pilot Project Award to S.M.P. and A.D.D., and a National Ataxia Foundation Postdoctoral Fellowship to C.J.A.

We thank D. Warren for kindly loaning a stimulus generator for the duration of our stimulation experiments.

Author Contributions

All authors contributed to study concept and design. C.J.A. contributed to data acquisition and analysis. C.J.A. and S.M.P. contributed to drafting the manuscript and figures.

Potential Conflicts of Interest

Nothing to report.

References

1. Pulst SM. Degenerative ataxias, from genes to therapies: the 2015 Cotzias lecture. Neurology 2016;86:2284–2290.
2. Banfi S, Servadio A, Chung MY, et al. Identification and characterization of the gene causing type 1 spinocerebellar ataxia. Nat Genet 1994;7:513–520.
3. Pulst SM, Nechiporuk A, Nechiporuk T, et al. Moderate expansion of a normally biallelic trinucleotide repeat in spinocerebellar ataxia type 2. Nat Genet 1996;14:269–276.
4. Bushart DD, Murphy GG, Shakkottai VG. Precision medicine in spinocerebellar ataxias: treatment based on common mechanisms of disease. Ann Transl Med 2016;4:25.
5. Lin CH, Wu YR, Kung PJ, et al. The potential of indole and a synthetic derivative for polyQ aggregation reduction by enhancement of the chaperone and autophagy systems. ACS Chem Neurosci 2014;5:1063–1074.
6. Takei A, Hamada S, Homma S, et al. Difference in the effects of tandospirone on ataxia in various types of spinocerebellar degeneration: an open-label study. Cerebellum 2010;9:567–570.
7. Zesiewicz TA, Greenstein PE, Sullivan KL, et al. A randomized trial of varenicline (Chantix) for the treatment of spinocerebellar ataxia type 3. Neurology 2012;78:545–550.
8. Lin XP, Feng L, Xie CG, et al. Valproic acid attenuates the suppression of acetyl histone H3 and CREB activity in an inducible cell model of Machado-Joseph disease. Int J Dev Neurosci 2014;38:17–22.
9. Kaut O, Jacobi H, Coch C, et al. A randomized pilot study of stochastic vibration therapy in spinocerebellar ataxia. Cerebellum 2014;13:237–242.
10. Hekman KE, Gomez CM. The autosomal dominant spinocerebellar ataxias: emerging mechanistic themes suggest pervasive Purkinje cell vulnerability. J Neurol Neurosurg Psychiatry 2015;86:554–561.
11. Kumar D, Timperley WR. The clinical, pathological and genetic aspects of sporadic late onset cerebellar ataxia: observations on a series of ten patients. Acta Neurol Scand 1988;77:181–186.
12. Oyama G, Thompson A, Foote KD, et al. Deep brain stimulation for tremor associated with underlying ataxia syndromes: a case series and discussion of issues. Tremor Other Hyperkinet Mov (N Y) 2014;4:228.
13. Hashimoto T, Muralidharan A, Yoshida K, et al. Neuronal activity and outcomes from thalamic surgery for spinocerebellar ataxia. Ann Clin Transl Neurol 2017;5:52–63.
14. Schvarcz JR, Sica RE, Morita E. Chronic self-stimulation of the dentate nucleus for the relief of spasticity. Acta Neurochir Suppl (Wien) 1980;30:351–359.
15. Teixeira MJ, Cury RG, Galhardoni R, et al. Deep brain stimulation of the dentate nucleus improves cerebellar ataxia after cerebellar stroke. Neurology 2015;85:2075–2076.
16. Machado AG, Baker KB, Schuster D, et al. Chronic electrical stimulation of the contralesional lateral cerebellar nucleus enhances recovery of motor function after cerebral ischemia in rats. Brain Res 2009;1280:107–116.
17. Baker KB, Schuster D, Cooperrider J, Machado AG. Deep brain stimulation of the lateral cerebellar nucleus produces frequency-specific alterations in motor evoked potentials in the rat in vivo. Exp Neurol 2010;226:259–264.
18. Figueroa KP, Paul S, Calì T, et al. Spontaneous shaker rat mutant—a new model for X-linked tremor-ataxia. Dis Model Mech 2016;9:553–562.
19. Erekat NS. Cerebellar Purkinje cells die by apoptosis in the shaker mutant rat. Brain Res 2017;1657:323–332.
20. Fowler SC, Birkestrand BR, Chen R, et al. A force-plate actometer for quantitating rodent behaviors: illustrative data on locomotion, rotation, spatial patterning, stereotypies, and tremor. J Neurosci Methods 2001;107:107–124.

21. Blumenfeld Z, Koop MM, Prieto TE, et al. Sixty-hertz stimulation improves bradykinesia and amplifies subthalamic low-frequency oscillations. Mov Disord 2017;32:80–88.
22. Kapural L, Yu C, Doust MW, et al. Novel 10-kHz high-frequency therapy (HF10 therapy) is superior to traditional low-frequency spinal cord stimulation for the treatment of chronic back and leg pain: the SENZA-RCT randomized controlled trial. Anesthesiology 2015;123: 851–860.
23. Pereira EAC, Aziz TZ. Neuropathic pain and deep brain stimulation. Neurotherapeutics 2014;11:496–507.
24. Engelhardt KA, Marchetta P, Schwarting RKW, Melo-Thomas L. Haloperidol-induced catalepsy is ameliorated by deep brain stimulation of the inferior colliculus. Sci Rep 2018;8:2216.
25. Umemura A, Oka Y, Yamamoto K, et al. Complications of subthalamic nucleus stimulation in Parkinson's disease. Neurol Med Chir (Tokyo) 2011;51:749–755.
26. King NO, Anderson CJ, Dorval AD. Deep brain stimulation exacerbates hypokinetic dysarthria in a rat model of Parkinson's disease. J Neurosci Res 2016;94:128–138.
27. Constantoyannis C, Kumar A, Stoessl AJ, Honey CR. Tremor induced by thalamic deep brain stimulation in patients with complex regional facial pain. Mov Disord 2004;19:933–936.
28. Grill WM, Snyder AN, Miocinovic S. Deep brain stimulation creates an informational lesion of the stimulated nucleus. Neuroreport 2004; 15:1137–1140.
29. Anderson CJ, Sheppard DT, Huynh R, et al. Subthalamic deep brain stimulation reduces pathological information transmission to the thalamus in a rat model of parkinsonism. Front Neural Circuits 2015; 9:31.
30. Agnesi F, Connolly AT, Baker KB, et al. Deep brain stimulation imposes complex informational lesions. PLoS One 2013;8:e74462.
31. Isaias IU, Volkmann J, Kupsch A, et al. Factors predicting protracted improvement after pallidal DBS for primary dystonia: the role of age and disease duration. J Neurol 2011;258:1469–1476.
32. Paxinos G, Watson C. *The Rat Brain in Stereotaxic Coordinates*. 6th ed. Waltham, MA: Academic Press, 2007.
33. Kuncel AM, Grill WM. Selection of stimulus parameters for deep brain stimulation. Clin Neurophysiol 2004;115:2431–2441.
34. Scoles DR, Meera P, Schneider MD, et al. Antisense oligonucleotide therapy for spinocerebellar ataxia type 2. Nature 2017;544:362–366.
35. Moore LR, Rajpal G, Dillingham IT, et al. Evaluation of antisense oligonucleotides targeting ATXN3 in SCA3 mouse models. Mol Ther Nucleic Acids 2017;7:200–210.
36. McConnell GC, So RQ, Hilliard JD, et al. Effective deep brain stimulation suppresses low-frequency network oscillations in the basal ganglia by regularizing neural firing patterns. J Neurosci 2012;32: 15657–15668.
37. Anderson T, Hu B, Pittman Q, Kiss ZH. Mechanisms of deep brain stimulation: an intracellular study in rat thalamus. J Physiol 2004;559 (pt 1):301–313.
38. Zucca R, Rasmussen A, Bengtsson F. Climbing fiber regulation of spontaneous Purkinje cell activity and cerebellum-dependent blink responses (1,2,3). eNeuro 2016;3. pii: ENEURO.0067-15.2015.
39. Birdno MJ, Grill WM. Mechanisms of deep brain stimulation in movement disorders as revealed by changes in stimulus frequency. Neurotherapeutics 2008;5:14–25.
40. Williams ER, Soteropoulos DS, Baker SN. Spinal interneuron circuits reduce approximately 10-Hz movement discontinuities by phase cancellation. Proc Natl Acad Sci U S A 2010;107:11098–11103.
41. McConnell GC, So RQ, Grill WM. Failure to suppress low-frequency neuronal oscillatory activity underlies the reduced effectiveness of random patterns of deep brain stimulation. J Neurophysiol 2016; 115:2791–2802.
42. Louis ED, Kuo SH, Tate WJ, et al. Heterotopic Purkinje cells: a comparative postmortem study of essential tremor and spinocerebellar ataxias 1, 2, 3, and 6. Cerebellum 2018;17:104–110.
43. Dietrichs E, Bjaalie JG, Brodal P. Do pontocerebellar fibers send collaterals to the cerebellar nuclei? Brain Res 1983;259:127–131.
44. Stone LS, Lisberger SG. Visual responses of Purkinje cells in the cerebellar flocculus during smooth-pursuit eye movements in monkeys. II. Complex spikes. J Neurophysiol 1990;63:1262–1275.
45. Ishikawa T, Tomatsu S, Tsunoda Y, et al. Releasing dentate nucleus cells from Purkinje cell inhibition generates output from the cerebrocerebellum. PLoS One 2014;9:e108774.
46. Heiney SA, Kim J, Augustine GJ, Medina JF. Precise control of movement kinematics by optogenetic inhibition of Purkinje cell activity. J Neurosci 2014;34:2321–2330.
47. Sugihara I, Wu H, Shinoda Y. Morphology of axon collaterals of single climbing fibers in the deep cerebellar nuclei of the rat. Neurosci Lett 1996;217:33–36.
48. Choe CU, Hidding U, Schaper M, et al. Thalamic short pulse stimulation diminishes adverse effects in essential tremor patients. Neurology 2018;91:e704–e713.
49. Hansen ST, Meera P, Otis TS, Pulst SM. Changes in Purkinje cell firing and gene expression precede behavioral pathology in a mouse model of SCA2. Hum Mol Genet 2013;22:271–283.
50. Benabid AL, Pollak P, Gervason C, et al. Long-term suppression of tremor by chronic stimulation of the ventral intermediate thalamic nucleus. Lancet 1991;337:403–406.